

The re-radiation estimate for 1950 is comparable to Kiehl et al. 1997 [2] value. In their assessment, they determined the total longwave GHG re-radiative of 155 W/m² and a clear sky re-radiation of 125 W/m². Given cloud coverage is roughly 67%, the weighted average is 145 W/m² in 1990. This is very close to the 147 W/m² estimate in Figure 1 due to the optimum 61.8% re-radiation condition derived in our model and illustrated in Figure 1. From the figure, the average absorbed albedo ‘Energy In’ is multiplied by the a 1.618 re-radiation factor to obtain the 384.93 W/m².

Applications of these models are provided between two different periods (1950 and 2019). In 2019 the model's transitions are not self-deterministic and the iterative transitional energy states converge quickly to the maximum forcing value. Since the atmosphere is dynamic, it can be helpful to view some of the iterative transition states. As the atmosphere is in flux, transitional states and their convergent condition can be identified to a maximum available GHG forcing value.

2. Data and Method

When initial solar absorption occurs, part of the long-wavelength radiation given off is re-radiated back to Earth as depicted in Figure 1. In the absence of forcing, we denote this average re-radiation fraction as \bar{f}_1 . This presents a simplistic but effective model where

$$P_{Total} = P_{\alpha} + P_{GHG} = P_{\alpha} + \bar{f}_1 P_{\alpha} = P_{\alpha} (1 + \bar{f}_1) = \sigma T_s^4 \quad \text{where } P_{\alpha} = \frac{S_o}{4} (1 - \alpha) \quad (1)$$

As depicted in Figure 1, P_{α} is the ‘Energy In’, P_{GHG} is the GHG re-radiation energy, P_{Total} is the ‘Total Energy’, T_s is the surface temperature, and $S_o=1361\text{W/m}^2$. As one might suspect, \bar{f}_1 turns out to be exactly β^4 in the absence of forcing, so that \bar{f}_1 is a redefined variable taken from the effective emissivity constant of the planetary system. We identify $1+\bar{f}_1=1.618034$ (see Section 2.2) as the optimal global average ‘albedo-GHG’ radiation factor (Table 1) since it is a combined effect of the re-radiation and solar input.

2.1 Estimating the Global Optimal Average Re-radiation Strength

In geoengineering, we are working with absorption and re-radiation, we can write

$$P_{Total} = \sigma T_s^4 = \sigma \left(\frac{T_{TOA}}{\beta} \right)^4 \quad \text{and} \quad P_{\alpha} = \sigma T_{\alpha}^4 = \sigma (\beta T_s)^4 \quad (2)$$

The definitions of $T_{\alpha}=T_e$, T_s and β are the emission temperature, surface temperature, and typically $\beta \approx 0.887$, respectively. Consider a time when there are **no forcing issues** causing warming trends. Then by conservation of energy, the equivalent power re-radiated from GHGs in this model is dependent on P_{α} with

$$P_{GHG} = P_{Total} - P_{\alpha} = \sigma T_s^4 - \sigma T_{\alpha}^4 \quad (3)$$

To be consistent with $T_{\alpha}=T_e$, typically $T_{\alpha} \approx 255^{\circ}\text{K}$ and $T_s \approx 288^{\circ}\text{K}$, then in keeping with a common definition of the global beta (the proportionality between surface temperature and emission temperature) for the moment $\beta=T_{\alpha}/T_s=T_e/T_s$.

This allows us to write the dependence

$$P_{GHG} = \sigma T_s^4 - \sigma T_{\alpha}^4 = \frac{\sigma T_{\alpha}^4}{\beta^4} - \sigma T_{\alpha}^4 = \sigma T_{\alpha}^4 \left(\frac{1}{\beta^4} - 1 \right) = \sigma T_{\alpha}^4 \left(\frac{1}{\bar{f}} - 1 \right) \quad (4)$$

Note that if $\beta^4=1$, there would be no GHG contributions. Here we set \bar{f} , the re-radiation parameter equal to β^4 . We can also define the blackbody re-radiated similarly by some fraction, say f_1 such that

$$P_{GHG} = \bar{f}_1 P_{\alpha} = \bar{f}_1 \sigma T_{\alpha}^4 \quad (5)$$

According to Equations 4 and 5, we require

$$P_{GHG} = \sigma T_{\alpha}^4 \left(\frac{1}{\bar{f}} - 1 \right) = \bar{f}_1 \sigma T_{\alpha}^4 = \bar{f} \sigma T_{\alpha}^4 \quad (6)$$

When $\bar{f} = \bar{f}_1$, the solution is derived from the quadratic expression

$$\bar{f}^2 + \bar{f} - 1 = 0 \text{ yielding } \bar{f} = 0.618034 = \beta^4, \beta = (0.618034)^{1/4} = 0.88664 \quad (7)$$

This is very close to the common value estimated for β and it was obtained through energy balance in the planetary system providing a self-determining assessment. In geoengineering, we can view the re-radiation as part of the albedo effect. Consistency with the Planck parameter is shown in Appendix A. We note the assumption $\bar{f} = \bar{f}_1$ only works if planetary energy is in balance without forcing. In Appendix B, Eq. 7 is derived in another way by balancing energy in and out of our global system showing full agreement with this result.

2.2 Method for Estimating Global Nominal Average Re-radiation Strength for 1950

Global warming can be exemplified by looking at two different periods. The model in Equation 1 can be applied for 1950 which we take as a pseudo baseline time period where we

- assume no forcing issues causing a warming trend in 1950, then combining Eq. 1 and 7, we are now able to write P_{Total} in terms of the ‘albedo-GHG’ factor

$$P_{\text{Total}_{1950}} = 1.618 P_{\alpha} \quad (8)$$

This provides a baseline number for our geoengineering estimates so that 1.618 becomes the 1950 albedo-GHG reference value. As Figure 1 illustrates, the re-radiation value (0.618) is close to the results of other authors [2]. This reference value, is constrained by energy balance in Eq. 6. The actual values in Figure 1 will be exemplified in Section 3 to 1950.

2.3 Method for Estimating Global Average Re-radiation Strength for 2019

Deviations from the nominal 61.8% optimum value due to dynamics in the atmosphere and/or GHG forcing in the industrial era are not self-deterministic (as found in Eq. 7). Figure 2 shows the time series iterative process that can be modeled. Series convergence is found. Figure 2 only shows 2 to 3 iterations. Table 1 provides n=10 time series iterations.

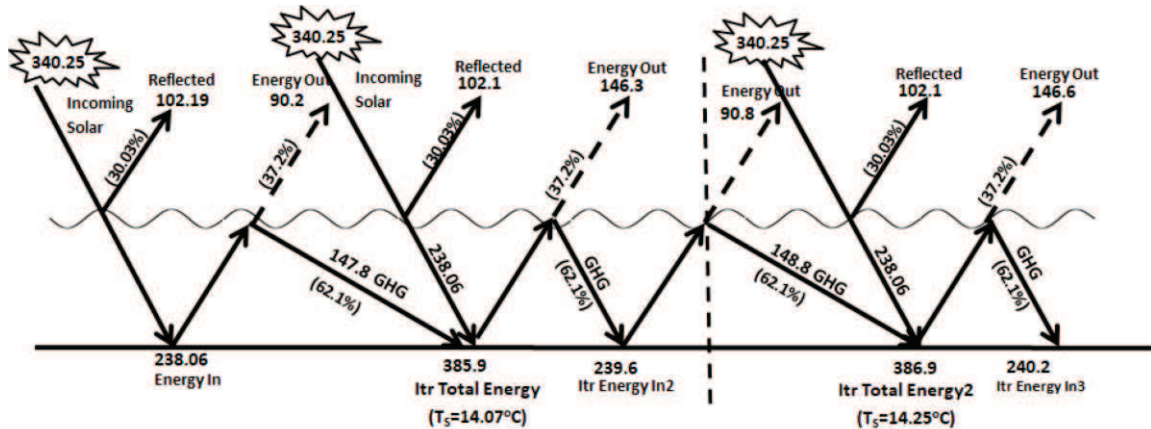


Figure 2 2019 GMEEB time series iterative re-radiation diagram (values in W/m^2)

Unlike feedback, which takes time to be realized due to the Earth's inertial, we do not expect much of an atmospheric lag in GHG forcing for a few reasons. In terms of GHG pollution, this builds up slowly over time (1950 to 2019). In terms of day-to-day changes, the transition states in Figure 2 converge fairly rapidly (see Table 1).

From Table 1, after 10 iterations, re-radiation stability is reached and the energy out (n=10) is equal to the energy in (n=1). At this point, Iterative (Itr) Energy Forcing has converged to $2.54 \text{ W}/\text{m}^2$ (n=10) (see Sec. 3) while the temperature has stabilized to 0.48°K (n=10) above the 1950 baseline period.

2.4 Method for Iterative Series Convergence in 2019 Transition States

Equation 1 can be written in the simplified iterative form for the 2019 re-radiation model (initially without feedback)

$$P_{\text{Total}_{2019}} = P_{\alpha'} + P_{\text{GHG}'} = P_{\alpha'}(1 + \bar{f}_2) \quad (9)$$

Here \bar{f}_2 is the average 2019 re-radiation value. From Figure 2 and Table 1, we determined the iterative time series solution for any transition final f_2 state as

$$f_{Sum} = \bar{f}_2 = \sum_{n=1}^N (f^{2n} + f^{2N+1}) \quad (10)$$

Table 1 Iterative Time Series Convergence

Quantity	Iteration Transitional States									
	n=1	n=2	n=3	n=4	n=5	n=6	n=7	n=8	n=9	n=10 Stable Maximum State
Itr Energy in (W/m ²)	238.1	239.6	240.2	240.5	240.5	240.6	240.6	240.6	240.6	240.6
Itr P _{GHG}	147.8	148.8	149.2	149.3	149.4	149.4	149.4	149.4	149.4	149.4
Itr Energy out (W/m ²)	90.2	90.8	91.1	91.1	91.2	91.2	91.2	91.2	91.2	91.2
Itr Energy2 out (W/m ²)	146.3	146.6	146.8	146.8	146.8	146.9	146.9	146.9	146.9	146.9
Total Energy Out (W/m ²)	236.5	237.5	237.8	238.0	238.0	238.0	238.1	238.1	238.1	238.1
Surface P Total 2019 (W/m ²)	385.9	386.9	387.2	387.4	387.4	387.4	387.45	387.46	387.46	387.46
Itr Forcing E (n=1)-E _{out} (W/m ²)	1.56	2.16	2.40	2.49	2.52	2.53	2.54	2.54	2.54	2.54
Tsurface rise 2019 (°K)	287.2	287.4	287.5	287.5	287.5	287.5	287.5	287.5	287.5	287.5
T rise above 1950 (°K)	0.18	0.36	0.43	0.46	0.47	0.47	0.47	0.46	0.48	0.48

The series must sum to \bar{f}_2 , an estimated average value according to Eq. 9. Analogous to Equation 5, the 2019 value is given by (see Sec. 3 for applications)

$$f_{2019} = \bar{f}_2 = \bar{f}_{1950} + \Delta\bar{f} = \bar{P}_{GHG_2019} / P_{\alpha_2019} \quad (11)$$

Table 2 shows f and its targeted time series convergence f_{sum} for 1950 and 2019. We added $f=0.60$ as an interesting transitional re-radiation state.

Table 2 $f_{SUM}(f)$ Values of Interest

Key Values	f	f_{Sum}
$f < \bar{f}_2$ 2019	0.620965	0.6276
$f = \bar{f}_1$ 1950	0.618	0.618
$f < \bar{f}_2$	0.60	0.563

As a check, note that if f is set to the optimal value $f=0.618$, then the series converges to the same value yielding $f_{sum}=0.618$, as expected, in agreement with the self-deterministic assessment found in Equation 7. Next, note that if $f < 0.618$, then $f_{sum} < f$ and if $f > 0.618$, then $f_{sum} > f$.

2.5 Energy Forcing Transition States and imbalance

In Table 1, Energy forcing is provided in Row 8. The interactive time series transitional convergent states for forcing is relative to 238.06 W/m² solar 'Energy In' and is found as

$$\begin{aligned} \Delta E_{Forcing} &= E_{in_n=10} - E_{in_n=1} = P_{\alpha} \cdot \left\{ \sum_{n=1}^N (f^{2n-1} + f^{2N}) - 1 \right\}_{f=0.620965} \\ &= 238.06 W / m^2 (1.0107 - 1) = 2.54 W / m^2 \end{aligned} \quad (12)$$

This forcing estimate is exemplified in Section 3 and in Table 3.

The energy imbalance, taken as the difference between $E_{in_n=1}$ and $E_{out_n=10}$, is equal to zero (Table 3).

3.0 Results

The re-radiation model may seem a bit confusing. However, in application, only Equations 1, 8, 9, and 13 are needed. These equations are incredibly simple but very helpful in geoengineering. While transitional states are illustrative and more formal, the main focus for presenting them is to support Figures 1 and 2 and the basic idea of the re-radiation convergence.

In 1950 we simplify estimates by assuming the re-radiation parameter is fixed and reasonably close to the optimum average value for $f_1=0.618$ in reasonable agreement with other authors [2]. Then, to obtain the 1950 average surface temperature, $T_{1950}=13.89^\circ\text{C}$ (287.04°K), the only adjustable parameter left in our model is the global albedo (see also Eq. 1). This requires an albedo value of 0.3008 (see Table 3) to obtain $T_{1950}=287.04^\circ\text{K}$. This albedo number is reasonable and similar to the values cited in the literature [3]. From these values, the 1950 GMEEB diagram in Figure 1 can be obtained. Given the incident solar radiation (340.25 W/m^2) and the albedo value, then 'Energy in' is $P_\alpha=237.9 \text{ W/m}^2$, and from Eq. 8, $P_{\text{Total}}=384.94 \text{ W/m}^2$, and $P_{\text{GHG}}=384.94 \text{ W/m}^2-237.9 \text{ W/m}^2=147.1 \text{ W/m}^2$ (Eq. 3). These values are summarized in row 3 in Table 3.

In 2019, we add a small albedo decline of 0.15% that the author has estimated in another study [6] due to surface reflectivity losses related to UHIs. This will also help provide insight in the albedo effect (see Sec. 4.2). Given the incident solar radiation (340.25 W/m^2) and the marginally lower albedo value, then 'Energy in' is slightly higher than 1950 at $P_\alpha'=238.06 \text{ W/m}^2$. Next, we use IPCC estimates for GHG forcing as a way to calibrate our model. We assume most of the forcing is due to IPCC/NOAA estimates for GHGs. We adjusted our model to obtain the IPCC GHG forcing estimate between 1950 and 2019 found in their table of about 2.38 W/m^2 [4, 5].

The GHG re-radiation forcing is described as f_{Sum} in Equation 9 and 10. When f_{Sum} is adjusted to 0.6276 in Eq. 9, then $P_{\text{Total } 2019} = 1.6276 \times 238.06=387.46 \text{ W/m}^2$ and $P_{\text{GHG}}=387.46-238.06=149.4 \text{ W/m}^2$, which is the GHG value shown in Column 7, and the required forcing value 2.38 W/m^2 [4, 5] relative to 1950 is obtained as required. In Table 3, the 2019 row is a summary without feedback. To incorporate feedback, an amplification factor is estimated as $A_F=1.98=0.95^\circ\text{C}/0.48^\circ\text{C}$. Therefore, the feedback is estimated on the known temperature change in 2019. Here we apply feedback as a separate term at the end in the last row in Table 3.

In general, feedbacks estimates are hard to quantify [7], our estimate is consistent with the temperature rise for 2019. We anticipate this could be larger due to the climate feedback inertia.

Table 3 Model Results

Year	$T_s(^{\circ}\text{K})$	$T_\alpha(^{\circ}\text{K})$	f_{1950}, f_{2019}	α, α'	P_α Energy In W/m^2	P_{GHG} P_{GHG}	P_{Total} W/m^2
2019	287.52	254.55	0.6276	30.03488	238.06	149.4	387.46
1950	287.04	254.51	0.6180	30.08	237.903	147.024	384.927
$\Delta_{2019-1950}$	0.48	0.043	0.0096	(0.15%)	0.157	2.38	2.54
$\Delta_{\text{Feedback } A_F=1.98}$	0.95	0.085	-	-	0.311	4.71	5.01

Row 3 in Table 3 indicated that the feedback amplification factor A_F has been incorporated into the forcing model in the following manner

$$P_{\text{Total } 2019 \& \text{ Feedback}} = P_{1950} + (\Delta P) A_F = P_{1950} + (P_{2019} - P_{1950}) A_F = \sigma T_S^4 \quad (13)$$

We note the forcing given by $\Delta P_{\text{GHG}}=2.38 \text{ W/m}^2$ when added to the albedo forcing change, yields a total forcing of $\Delta P_{\text{Total}}=2.54 \text{ W/m}^2$. Figure 3 illustrates the 2019 GMEEB for the $n=10$ transitional state. Note the forcing is estimated from Fig. 3 as the difference in the 'Energies In', $240.6 \text{ W/m}^2-238.06 \text{ W/m}^2=2.54 \text{ W/m}^2$. The re-radiation may be obtained using $f=0.621$ or $f_{\text{sum}}=0.6276$ (see Eq. 10) as indicated in the Figure 3 diagram. Note the imbalance for the Energy In – Energy Out=0 relative to $n=1$ $E_{in}=238.06 \text{ W/m}^2$. We note that unlike f_{1950} , f_{2019} is not a strict measure of the emissivity due to the increase in GHGs (see Eq. A-3).

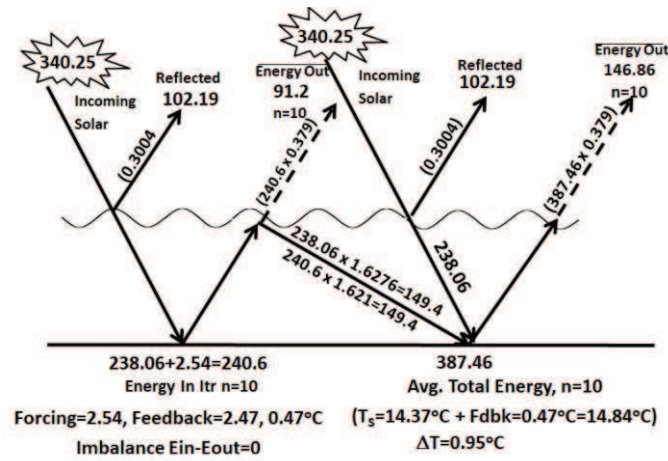


Figure 3 2019 GMEEB re-radiation convergent diagram with forcing & feedback from Table 3, $n=10$ (in W/m^2)

4.0 Discussion on the Importance of the Albedo Solution to Global Warming

Policymakers should recognize the need for albedo management in global warming mitigation. Although albedo solutions have been recommended in helping to mitigate climate change [1, 8-16] and likely a vital supplement to CO₂ efforts, little work is being done in this area. There have been several proposed albedo solutions, both surface and atmospheric methods [1, 8-16] to reduce climate change. Such techniques have not been widely adopted by governments [15], typically given little funding consideration, and were not part of the Paris Climate Accord [17]. Because of the poor focus on the albedo solution, in this section, we felt compelled to point out several advantages supported by this paper.

4.1 The GHG Interaction Albedo Advantage

From Table 1 or Figure 1 and 2, the 'Energy In' is effectively increased by 'albedo-GHG' re-radiation 1.62 factor. For example, in 1950 the surface energy is

$$1.618 \times 287.9 \text{ W/m}^2 = 384.9 \text{ W/m}^2 \quad (14)$$

Effectively, the 1.62 albedo-GHG factor, is a combined effect of solar radiation and GHG re-radiation, therefore it is of course higher than the GHGs re-radiation itself. That is, in terms of a mitigation strategy, reverse GHG forcing requires the full 2.38 W/m^2 , while the albedo-GHG re-radiation compounding effect (with the same albedo for 2019), shows that albedo reverse forcing would only requires 1.46 $Watts/m^2$, i.e.,

$$1.618 \times 1.47 \text{ W/m}^2 = 2.38 \text{ W/m}^2 \quad (15)$$

This albedo-GHG advantage can be illustrated in Equation 1 and 12 by the rate of change for P_{Total} where

$$\left(\frac{dP_{Total}}{dP_{\alpha}} \right)_{1950} = (1 + f_1) = 1.618 \quad \text{and} \quad \left(\frac{dP_{Total}}{dP_{\alpha}} \right)_{2019} = (1 + f_2) = 1.6276 \quad (16)$$

However, the rate of change due to GHGs is only

$$\frac{dP_{Total}}{dP_{GHG}} = \frac{d(P_{\alpha} + P_{GHG})}{dP_{GHG}} = 1 \quad (17)$$

This helps demonstrate this concept, its clear advantage and importance for albedo controls in global warming mitigation strategies due to the albedo-GHG factor.

A simple way for policymakers to remember and understand this advantage can be illustrated in the following fundamental statements:

- *Increasing the reflectivity of a hotspot surface reduces its greenhouse gas effect*
- *Decreasing the reflectivity of a hotspot surface increases its greenhouse gas effect*

- *The Global Warming change associated with a reflectivity hotspot modification is given by the albedo-GHG radiation factor having an approximate average value of 1.62.*

4.2 Percent Albedo Change Required for Reverse Forcing

From Table 1, a useful albedo-gamma parameter is observed denoted as

$$\gamma_{\% \Delta \alpha} = \frac{(\Delta E_o)_\alpha}{\frac{\alpha_1 - \alpha_2}{\alpha_1} 100} = \frac{0.157 W / m^2}{0.15 \% \Delta \text{albedo}} \approx 1 W / m^2 / \% \Delta \text{albedo} \quad (18)$$

This gamma albedo value is a simple number and can be applied to Equation 15 results for reverse forcing assessment that indicates the required percent albedo change

$$\text{Reverse Forcing \% Albedo Change} = 1.47 W / m^2 / 1 W / m^2 / \% \Delta \text{albedo} = 1.47 \% \quad (19)$$

The albedo-gamma parameter in Equation 18 can be derived more formally by considering an albedo change from two different periods. Here a global albedo change from α_1 to α_2 results as following [1]

$$\gamma_{\% \Delta \alpha} = \frac{(\Delta S_o)_\alpha}{\frac{\alpha_1 - \alpha_2}{\alpha_1} 100} = \frac{S_o (\alpha_1 - \alpha_2)}{\frac{\alpha_1 - \alpha_2}{\alpha_1} 100} = E_o \alpha_1 / 100 \approx 1 W / m^2 / \% \Delta \text{albedo} \quad (20)$$

Considering the incoming solar radiation $S_o \approx 340.25 W/m^2$ and letting $\alpha_1 \approx 0.294$, the value observed value for the albedo-gamma parameter is approximately $1.0 W/m^2 / \Delta \% \text{albedo}$.

4.3 Global Warming Albedo Solution Advantages for Humidity

Mitigating global warming has several advantages in the area of humidity feedback and forcing problems. Many of these advantages could be realized if the reflectivity of Urban Heat Islands (UHI) could be increased. One important advantage is for UHI in humid areas. Here we identify three main humidity effects that require albedo management.

1. Zhao et al. [18] observed that UHI temperatures increase in daytime ΔT by $3.0^\circ C$ in humid climates but decrease ΔT by $1.5^\circ C$ in dry climates. They found a strong correlation between ΔT increase and daytime precipitation. Their results concluded that albedo management would be a viable means of reducing ΔT on large scales.

This effect is often attributed to greenspace decrease of surface roughness due to UHI impermeable smooth surfaces which reduces convection cooling efficiency (Zhao et al. [18], Gunawardena et al [19]). However, UHIs create high evaporation rates and therefore some degree of convection cooling. Therefore, another possible reason we might consider is related to the fact that the air over cities is warmer and since warm air holds more water vapor, this could promote a local GHG effect and be partly responsible for the observed warming. These effects may to a lesser extent to all smooth hot evaporating surfaces (during precipitation periods) including roads and highways. Nevertheless, the primary mitigating factor in all these cases would be albedo management of impermeable surfaces.

2. From the change in the GMEEB, the Earth's temperature has increased since 1950 from $287.04^\circ K$ to $287.52^\circ K$ in 2019. Since warmer air holds more water vapor, a crude estimate of this water vapor increase is about 345 ppmv (by volume) or 205 PPM by weight [20] at an average global mean relative humidity of 70%RH [21]. This represents a factor of 3.4 times larger increase compared to CO_2 which has increased about 100ppmv since 1950, changing from 312ppmv to 412ppmv in 2019 [22]. This creates a very large warming feedback GHG water vapor effect, as suggested by Dessler [23] or Manabe et al. [24]. This is a very large effect. This important needed reduction of the atmospheric water vapor that is accumulating can only be accomplished through cooling and reversing trends, Therefore we need improvements for both GHG pollutions reduction and UHI albedo controls [1, 6].
3. Cao et. al. [25] did a study on wetland reduction in China and its correlation to drought with the following conclusion, "The wetland distributions and areas of the five provinces of southwestern China in the 1970s, 1990, 2000 and 2008 show that the total reduction of wetland area in the five provinces of southwestern China from 1970 to 2008, accounting for about 17% of the ground area with a higher rate from 2000 to 2008. They found the changes to the wetland area showed a negative correlation with temperature (i.e.

wetland decrease, increase in temperature), and a positive correlation with precipitation (i.e. wetland decrease, precipitation decrease).” One can conclude that albedo management of UHIs would help increase condensation. Although some cities find increases in precipitation due to complex warming turbulence, the larger picture indicates that UHI are a cause of drought.

As concluded by Zhou et al. [18], albedo management is likely an important aspect of UHI global warming humidity mitigation issues.

4.0 Conclusion

In this paper, an alternate way to view the GMEEB is provided using re-radiation modeling. This presented several unique ways the GMEEB can be viewed and insights suggested goengineering assessment methods and climate change albedo mitigation strategies.

We found in modeling a self-deterministic optimum pre-industrial global mean re-radiation factor of 0.618 which allows for energy balance (see Fig. 1) without requiring transitional convergent states. The parameter can be taken as a redefined variable of the effective emissivity constant for the planetary system ($\beta^4=0.618$). This allows one to estimate either the Earth's albedo or surface temperature when one of these is known. We applied this factor to 1950 as a pseudo-pre-industrial year. Since the energy in is dictated by the Earth's albedo and is increase by the GHG re-radiation by a factor of 1.618, we denoted this value as the albedo-GHG factor for 1950.

Re-radiation values outside this optimum factor required convergent transitional states. A convergent series solution was found. However, the model, in general, is easy to apply and was provided for 2019 with forcing and feedback considerations. In the present day, the mean re-radiation factor was found to increase to 0.6276 due to GHGs forcing

Because of the already numerous activities on-going in CO₂ and other GHG reduction, we focused on providing insights for albedo solutions. In this case, we noted that the mitigation required to offset the warming that occurred from 1950 to 2019 requires a GHG reverse forcing of 2.38 W/m² compared to a 1.47 W/m² albedo reduction. This is a 1.62 reduction, due to the ‘albedo-GHG’ factor. We also identified an albedo-gamma parameter equal to 1 W/m²/% Δ albedo. The albedo-gamma parameter applied to the 1.47 W/m² value indicates an albedo change of approximately 1.47% global reflectivity increase would be required to mitigate the warming that has occurred since 1950.

Lastly, we noted that UHI albedo management would have important benefits related to humidity climate change effects. These include reducing the warming humidity effect in cities, drought reduction, and lowering GHG local atmospheric water vapor through cooling while likely also increasing convection cooling.

The following albedo management suggestions and corrective actions are recommended:

- Modification of the Paris Climate Agreement to include albedo controls and solutions
- Albedo guidelines for both UHIs and roads similar to on-going CO₂ efforts
- Guidelines for future albedo design considerations of cities
- Government money allocation for goengineering and implement albedo solutions
- Task an agency like NASA to find applicable albedo solutions and implementing them
- Requires cars to be more reflective. Although world-wide vehicles likely do not embody much of the Earth's area, recommending that all newly manufactured cars are higher in reflectivity (e.g., silver or white) would help raise awareness of this issue similar to electric automobiles that help improve CO₂ emissions.

Appendix A: Re-radiating Model Consistency with Beta and the Planck Parameter

It is of interest to show model consistency with beta as it is tied to the re-radiation factor (see Eq.4). Using temperatures obtained from modeling in Table 3 from the two different periods (see Eq. A-3) we note

$$\beta_{1950} = \frac{T_a}{T_s} = \frac{T_{TOA}}{T_s} = \frac{254.51}{287.04} = 0.88667 \text{ and } \beta_{1950}^4 = 0.61809 \quad (\text{A-1})$$

And in 2019

$$\beta_{2019} = \frac{T_a}{T_s} = \frac{T_{TOA}}{T_s} = \frac{254.55}{287.5} = 0.885 \text{ and } \beta_{2019}^4 = 0.6145 \quad (\text{A-2})$$

These values are reasonably consistent. We also note that

$$f_{2019} = \beta_{2019}^4 + \Delta f \approx f_{1950} + \Delta f = \beta_{1950}^4 + \Delta f = 0.618 + 0.0096 = 0.6276 \quad (\text{A-3})$$

The 0.0096 value is noted in Table 3. This yields the expected re-radiation factor $f_{2019}=0.6276$.

The re-radiation model also is consistent with the Planck parameter. Results in Table 3, show the following estimates for the Planck parameter [27]

$$\lambda_o = -4 \frac{\Delta R_{LWR}}{T_s} = -4 \left(\frac{237.9W/m^2}{287.04^\circ K} \right)_{1950} = -3.315W/m^2/^\circ K \quad (\text{A-4})$$

and

$$\lambda_o = -4 \frac{\Delta R_{LWR}}{T_s} = -4 \left(\frac{238.06W/m^2}{287.5^\circ K} \right)_{2019} = -3.312W/m^2/^\circ K \quad (\text{A-5})$$

We note these are very close in value showing minor error and consistency with Planck parameter value, often taken as $-3.3W/m^2/^\circ K$ [27].

Appendix B: Balancing P_{out} and P_{in} in 1950

Although f_1 has been uniquely defined in Eq. 7, this should also result from balancing the energy in and out of the GMEEB. In equilibrium, the radiation that leaves must balance P_α energy in. Then from the GMEEB in Figure 1

$$\begin{aligned} Energy_{Out} &= (1-f_1)P_\alpha + (1-f_1)P_{Total} = (1-f_1)P_\alpha + (1-f_1)\{P_\alpha + f_1P_\alpha\} \\ &= 2P_\alpha - f_1P_\alpha - f_1^2P_\alpha = Energy_{in} = P_\alpha \end{aligned} \quad (\text{B-1})$$

This is consistent, so that in 1950 Eq. B-1 requires the same quadratic solution as Eq. 7. It is also apparent that

$$P_\alpha = \frac{P_{Total_1950}}{1+f_1} = f_1 P_{Total_1950} = \beta_1^4 P_{Total_1950} \quad (\text{B-2})$$

since

$$f_1 = \frac{1}{1+f_1} \quad (\text{B-3})$$

also yields Eq. 7. As a final check, an application in Section 3, Table 3 results, and illustrates that f_1 provides reasonable results.

Disclosures

Funding: This study was unfunded.

Conflicts of Interest: The author declares that there are no conflicts of interest.

References

1. Feinberg A., On Geoengineering and Implementing an Albedo Solution with UHI GW and Cooling Estimates vixra 2006.0198, DOI: 10.13140/RG.2.2.26006.37444/6 (Currently in Peer Review in the J. Mitigation and Adaptation Strategies for Global Change)
2. Kiehl, J.T. and Trenberth, K.E., 1997: Earth's Annual Global Mean Energy Budget. Bull. American Meteorological Society, Vol.78, 197–208
3. Stephens G., O'Brien D., Webster P, Pilewski P, Kato S, Li J, (2015) The albedo of Earth, *Rev. of Geophysics*, <https://doi.org/10.1002/2014RG000449>
4. Butler J., Montzka S., (2020) The NOAA Annual Greenhouse Gas Index, Earth System Research Lab. Global Monitoring Laboratory, <https://www.esrl.noaa.gov/gmd/aggi/aggi.html>
5. Wikipedia, Radiative forcing (2020)
6. Feinberg A, (2020) Urban Heat Island Amplification Estimates on Global Warming Using an Albedo Model, Vixra 2003.0088, DOI: 10.13140/RG.2.2.32758.14402/15 (Currently under peer review in the journal SN Applied Science)
7. IPCC, 2018: Global Warming of 1.5°C. An IPCC Special Report on the impacts of global warming of 1.5°C above pre-industrial levels and related global greenhouse gas emission pathways, in the context of strengthening the global response to the threat of climate change, sustainable development, and efforts to

- eradicate poverty [Masson-Delmotte, V., P. Zhai, H.-O. Pörtner, D. Roberts, J. Skea, P.R. Shukla, A. Pirani, W. Moufouma-Okia, C. Péan, R. Pidcock, S. Connors, J.B.R. Matthews, Y. Chen, X. Zhou, M.I. Gomis, E. Lonnoy, T. Maycock, M. Tignor, and T. Waterfield (eds.)].
8. Dunne D, (2018) Six ideas to limit global warming with solar geoengineering, CarbonBrief, <https://www.carbonbrief.org/explainer-six-ideas-to-limit-global-warming-with-solar-geoengin>
 9. Pattyn F., Ritz C., Hanna E., Asay-Davis X., DeConto R., Durand G., Favier L., Fettweis X., Goelzer H., Golledge N., Munneke P., Lenaerts J., Nowicki S, Payne A., Robinson A., Seroussi H., Trusel L., Broeke M., (2018) The Greenland and Antarctic ice sheets under 1.5 °C global warming, *Nature Climate Change*
 10. Koen G. Helwegen1 , Claudia E. Wieners, A, Jason E. Frank L, and Henk A. Dijkstra, Complementing CO2 emission reduction by solar radiation management might strongly enhance future welfare, (2019) *Earth System Dynamics*
 11. Latham, J., Rasch, P., Chen, C.-C., Kettles, L., Gadian, A., Gettelman, A., Morrison, H., Bower, K., and Choulaton, T.: Global temperature stabilization via controlled albedo enhancement of low-level maritime clouds, *Philos. T. R. Soc. A*, 366, 3969–3987, <https://doi.org/10.1098/rsta.2008.0137>, 2008.
 12. Ahlm, L., Jones, A., Stjern C, Muri, H., Kravitz, B., and Kristjánsson, J. E.: Marine cloud brightening – as effective without clouds, *Atmos. Chem. Phys.*, 17, 13071–13087, <https://doi.org/10.5194/acp-17-13071-2017>, 2017
 13. Gabriel, C. J., Robock, A., Xia, L., Zambri, B., and Kravitz, B.: The G4 Foam Experiment: global climate impacts of regional ocean albedo modification, *Atmos. Chem. Phys.*, 17, 595–613, <https://doi.org/10.5194/acp-17-595-2017>, 2017
 14. Seneviratne, S. I., Phipps, S. J., Pitman, A. J., Hirsch, A. L., Davin, E. L., Donat, M. G., Hirschi, M., Lenton, A., Wilhelm, M., and Kravitz, B.: Land radiative management as contributor to regional-scale climate adaptation and mitigation, *Nat. Geosci.*, 11, 88–96, <https://doi.org/10.1038/s41561-017-0057-5>, 2018.
 15. Cho A, (2016) To fight global warming, Senate calls for a study of making Earth reflect more light, *Science*, <https://www.sciencemag.org/news/2016/04/fight-global-warming-senate-calls-study-making-earth-reflect-more-light>
 16. Levinson, R., Akbari, H. (2010) Potential benefits of cool roofs on commercial buildings: conserving energy, saving money, and reducing the emission of greenhouse gases and air pollutants. *Energy Efficiency* 3, 53–109. <https://doi.org/10.1007/s12053-008-9038-2>
 17. Paris Climate Accord, (2015) <https://unfccc.int/process-and-meetings/the-paris-agreement/what-is-the-paris-agreement>
 18. Zhao L., Lee X, Smith R., Oleson K. (2014) Strong, contributions of local background climate to urban heat islands, *Nature*. 10;511(7508):216-9. DOI: 10.1038/nature13462
 19. Gunawardena K, Wells M, Kershawa T (2017) Utilising green and blue space to mitigate urban heat island intensity, *ScienceDirect*, doi: 10.1016, <https://www.sciencedirect.com/science/article/pii/S0048969717301754>
 20. Calculator.net, Dew Point Calculator, <https://www.calculator.net/dew-point-calculator.html?airtemperature=287.04&airtemperatureunit=kelvin&humidity=70&dewpoint=&dewpointunit=fahrenheit&x=60&y=24>
 21. Center for Sustainability and the Global Environment, Average Annual Relative Humidity, <https://nelson.wisc.edu/sage/data-and-models/atlas/data.php?incdataset=Average%20Annual%20Relative%20Humidity>
 22. NASA CO2 Database used for 1951, <https://data.giss.nasa.gov/modelforce/ghgases/Fig1A.ext.txt>, <https://climate.nasa.gov/vital-signs/carbon-dioxide/>
 23. Dessler A., Zhang Z., Yang P., (2008) Water-vapor climate feedback inferred from climate fluctuations, 2003–2008, *Geophysical Research Letters*, <https://doi.org/10.1029/2008GL035333>
 24. Manabe, S., and R. T. Wetherald (1967), Thermal equilibrium of the atmosphere with a given distribution of relative humidity, *J. Atmos. Sci.*, 24, 241–259
 25. C.X. Cao, J. Zhao, P. Gong, G. R. MA, D.M. Bao, K.Tian, Wetland changes and droughts in southwestern China, *Geomatics, Natural Hazards and Risk*, Oct 2011, <https://www.tandfonline.com/doi/full/10.1080/19475705.2011.588253>
 26. Kimoto K., (2006) On the Confusion of Planck Feedback Parameters, *Energy & Environment* (2009)